Lab on a Chip

RSC Publishing

PAPER

View Article Online
View Journal | View Issue

Published on 12 March 2013. Downloaded by University of Toronto on 04/06/2013 21:33:14.

Cite this: *Lab Chip*, 2013, **13**, 2591

A 3D microfluidic platform incorporating methacrylated gelatin hydrogels to study physiological cardiovascular cell–cell interactions

Michelle B. Chen,[a] Suthan Srigunapalan,[ab] Aaron R. Wheeler[bc] and Craig A. Simmons*[ab]

The cardiovascular system is particularly well-suited to modelling with microfluidic technologies, and much progress has been made to create microfluidic devices that mimic the microvasculature. In contrast, microfluidic platforms that model larger blood vessels and heart valves are lacking, despite the clear potential benefits of improved physiological relevance and enhanced throughput over traditional cell culture technologies. To address this need, we developed a bilayer membrane microfluidic device to model the vascular/valvular three-dimensional environment. Key features of the platform include physiologically-relevant spatial arrangement of multiple cell types, fluid flow over an endothelial monolayer, a porous membrane that permits heterotypic cell interactions while maintaining cell compartmentalization, and a photopolymerizable gelatin methacrylate (gel-MA) hydrogel as a physiologically-relevant subendothelial 3D matrix. Processing guidelines were defined for successful in-channel polymerization of gel-MA hydrogels that were mechanically stable, had physiologically-relevant elastic moduli of 2–30 kPa, and supported over 80% primary cell viability for at least four days in culture. The platform was applied to investigate shear stress-regulated paracrine interactions between valvular endothelial cells and valvular interstitial cells. The presence of endothelial cells significantly suppressed interstitial cell pathological differentiation to α-smooth muscle actin-positive myofibroblasts, an effect that was enhanced when the endothelium was exposed to flow-induced shear stress. We expect this versatile organ-on-a-chip platform to have broad utility for mechanistic vascular and valvular biology studies and to be useful for drug screening in physiologically-relevant 3D cardiovascular microenvironments.

Received 10th January 2013,
Accepted 12th March 2013

DOI: 10.1039/c3lc00051f

www.rsc.org/loc

Introduction

Microfluidic cell culture technologies offer great promise for the creation of *in vitro* microenvironments that closely mimic those found *in vivo*.[1] Among the essential characteristics required to achieve physiologically-relevant microfluidic platforms is the incorporation of three-dimensional (3D) cellular microenvironments. These are typically characterized by the presence of interacting heterotypic cells types in a proper spatial arrangement, which often involves encapsulation of at least one cell type within a 3D extracellular matrix (ECM).

A good example of this, and one that is particularly well-suited to study with microfluidic technologies,[2,3] is the vascular system. The vascular microenvironment consists of a 3D ECM embedded with smooth muscle cells, pericytes, and/or fibroblasts that surrounds conduits lined on their inner surface with a monolayer of endothelial cells (ECs); the ECs are exposed to blood flow-induced shear stress and circulating blood cells and macromolecules. Much progress has been made to create microfluidic 3D cell culture platforms that model vascular networks. Owing to the length scale similarity between microvessels and microfluidic channels, many applications to date have focused on microcirculatory phenomena, including microvascular hemodynamics, thrombosis, angiogenesis, and microvascular network formation for perfusion of engineered tissues (recently reviewed by Wong *et al.*[3]). Less focus has been given to developing microfluidic models of larger vessels, like arterioles and arteries, or similar cardiovascular structures, like heart valves. This is in part because macroscale cell culture systems (*e.g.*, parallel plate flow chambers) have been used successfully to investigate phenomena like the role of fluid shear in vascular and valvular diseases.[4–6] However, microfluidic systems offer the major advantage of enhanced throughput, and as such the development of microfluidic models that permit the study of vascular/

[a]*Department of Mechanical and Industrial Engineering, University of Toronto, 5 King's College Road, Toronto, Ontario, Canada M5S 3G8. E-mail: c.simmons@utoronto.ca; Fax: +1 416 978 7753; Tel: +1 416 946 0548*
[b]*Institute of Biomaterials and Biomedical Engineering, University of Toronto, 164 College Street, Toronto, Ontario, Canada M5S 3G9*
[c]*Department of Chemistry, University of Toronto, 80 St. George Street, Toronto, Ontario, Canada M5S 3H6*

This journal is © The Royal Society of Chemistry 2013

Published on 12 March 2013. Downloaded by University of Toronto on 04/06/2013 21:33:14.

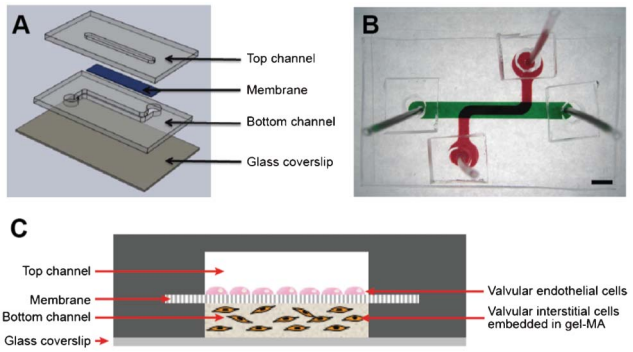

Fig. 1 (A) Schematic and (B) photograph of bilayer membrane microfluidic device. The scale bar in panel (B) is 5 mm. (C) Cross-sectional schematic illustrating the spatial arrangement of the cells in the device. Cell culture media is flowed in the top channel in the direction into the page in this schematic.

valvular phenomena (*e.g.*, vasomotion) has been identified as a priority.[3]

A challenge to the development of such systems is that the biomaterials used in many of the microvascular microfluidic platforms (often type I collagen) are not readily tuned to mimic the native ECM and suffer from poor mechanical stability that preclude them from being used for long-term culture of vascular smooth muscle cells or valvular interstitial cells (VICs), which readily contract and degrade natural ECMs. Moreover, EC sprouting occurs in many microvascular microfluidic systems that incorporate 3D gels because these devices lack the basement membrane that compartmentalizes ECs and mural cells and regulates vascular sprouting *in vivo*.

To address these challenges, we previously developed a bilayer membrane microfluidic platform to mimic the vascular/valvular microenvironment. The device consists of upper and lower microchannels that are separated by a porous membrane (Fig. 1). The membrane compartmentalizes the upper "luminal" channel and the lower "mural" channel while permitting passage of macromolecules and extravasating cells. This platform has been used to study endothelial permeability[7] and EC–leukocyte interactions under fluid shear;[8] in both cases, ECs were grown on the membrane in the top channel, but the bottom channel was left empty.

Here we advance this platform by incorporating a cell-laden hydrogel in the bottom channel to more fully mimic the vascular/valvular microenvironment. We selected photopolymerizable gelatin methacrylate (gel-MA) as the hydrogel as it retains the natural cell binding motifs and degradability of native collagen but has superior mechanical properties, which are tunable.[9] It has also been shown to support VIC function over several weeks in macroscale culture.[10] We present guidelines for the successful incorporation and customization of gel-MA into microfluidic devices by characterizing the hydrogel mechanical properties and determining processing parameters that support primary cell viability. Finally, we demonstrate the utility of the platform to study shear-regulated interactions between valvular endothelial cells (VECs) and VICs. Calcific aortic valve disease, a common disorder that currently has no medical treatment,[11] is associated with the pathological differentiation of fibroblast-like VICs into myofibroblasts that cause fibrosis. VECs are believed to regulate VIC fate through paracrine signals that are hemodynamically regulated.[12,13] The microfluidic device presented here recapitulates these critical features of the valvular microenvironment and has the potential to enhance throughput over comparable macroscale technologies, and therefore may facilitate efforts to discover pharmacological therapies for valvular diseases.

Experimental methods

All reagents were purchased from Sigma-Aldrich (Oakville, ON, Canada) unless otherwise noted.

Microfluidic devices design and fabrication

Two sets of devices were used in this study: single layer microchannel devices and bilayer membrane microchannel devices. The single layer devices were used for characterization of hydrogel polymerization conditions and cell viability. S-shaped channels with cross-sectional dimensions of 2000 μm wide by 302 μm high were fabricated from polydimethylsiloxane (PDMS; Sylgard 184; Dow Corning, Midland, MI) using standard soft lithography. PDMS slabs and glass slides were plasma treated and bonded together to form a closed channel.

Bilayer membrane microchannel devices were used to study cell-cell interactions under fluid flow conditions (Fig. 1). To fabricate membrane devices, the top microchannel (4000 μm wide by 253 μm high) was formed with PDMS using standard lithography. The bottom S-shaped channel (2000 μm wide by 300 μm high) was formed *via* squeeze fabrication with aluminium moulds.[14] Moulds were filled with PDMS and excess PDMS was squeezed out to obtain a thin flat slab with a void region in the shape of the feature. A polyethylene terephthalate, track-etched porous membrane with 1 μm diameter pores was cut out from a standard cell culture insert (Becton Dickinson, Mississauga, ON, Canada) and bonded between the two PDMS channels, which had each been coated with a thin mortar layer of uncured PDMS *via* stamping.[7,8] Finally, the bottom channel was bonded to a thin plasma-treated glass No. 1.5 coverslip.

Synthesis and preparation of gel-MA

Type A porcine skin gelatin was mixed (10% w/v) into phosphate-buffered saline (PBS) at 65 °C and stirred on a stir plate until fully dissolved. To achieve a high degree of methacrylation, 0.8 g mL^{-1} of 94% methacrylic anhydride was added for every gram of gelatin at a rate of 0.5 mL min^{-1}. The mixture was left to react for 3 h while stirring at 50 °C. To stop the methacrylation reaction, 20 mL of PBS/g of gelatin was added. The synthesized solution was transferred to dialysis tubing and dialyzed for one week against deionized water at 50 °C in order to remove the methacrylic acid and other impurities. The gel-MA was then filtered, snap frozen with liquid nitrogen, and lyophilized for one week. Gel-MA product was used without further purification.

 This journal is © The Royal Society of Chemistry 2013

Published on 12 March 2013. Downloaded by University of Toronto on 04/06/2013 21:33:14.

Working pre-polymer solutions were prepared by mixing freeze dried gel-MA macromer of varying weight-volume percentages into PBS containing 2-hydroxy-1-(4-(hydroxyethoxy)phenyl)-2-methyl-1-propanone (Igracure 2959) as a photoinitiator at various concentrations and 80 °C until fully dissolved. Gel-MA pre-polymer was polymerized by exposure to 7.2 mW cm^{-2} UV light (360–480 nm) using a spot curing lamp (Omnicure S2000; Lumen Dynamics, Mississauga, ON, Canada).

Characterization of gel-MA mechanical properties

The modulus of elasticity of various gel-MA formulations was determined by compression testing. Moulds for gel-MA samples were made by punching 5 mm diameter discs out of a 1 mm-thick sheet of PDMS. Twenty microliters of uncured gel-MA of 5%, 10% and 15% (w/v) macromer concentrations with 0.5% (w/v) photoinitiator was pipetted into each well and sandwiched between two sheets of Teflon to remove air bubbles. After up to 30 s of UV polymerization, samples were gently removed from the mould and washed with PBS immediately before mechanical testing. Samples were loaded onto a mechanical tester (840LE2; TestResources Inc., Shakopee, MN) with a 1000 g load cell and were tested at a rate of 20% strain/min to a maximum load of 30 g. The compressive modulus was calculated as the slope of the linear region from 0% to 5% strain by converting load and displacement values into engineering stress and strain using the original cross sectional area and thickness of the sample.

Porosity of gel-MA hydrogels was determined using variable pressure (environmental) scanning electron microscopy (SEM) (Hitachi S-3400N). Hydrogel samples with 5%, 10% and 15% (w/v) gel-MA macromer concentration and 0.5% (w/v) photoinitiator were prepared in the form of 20 μL droplets on coverslips. Prior to imaging, the samples were flash frozen in liquid nitrogen and fractured to reveal the sample cross-section. Specimens were mounted on a cold stage covered in double-sided carbon tape for imaging. Pore diameters of the gels were calculated from the SEM images using NIH ImageJ software.

Cell encapsulation and culture in gel-MA in microfluidic devices

Primary porcine aortic valvular interstitial cells (VICs) were isolated by enzymatic digestion, subcultured, and frozen, as described previously.[15] Passage 3 VICs were thawed and cultured in Dulbecco's modified essential medium (DMEM), supplemented with 10% fetal bovine serum (FBS) (Fisher Scientific, Ottawa, ON, Canada) and 1% penicillin–streptomycin (P–S), for two days. VICs were then trypsinized, resuspended, and mixed in a 1 : 1 ratio with a macromer solution of 5%, 10% or 15% (w/v) gel-MA that had been warmed in a 37 °C bath. The cell/macromer solution was then injected into S-shaped (bottom) channel of the single layer or membrane microfluidic devices. The inlet and outlet ports were masked by aluminum foil to prevent curing of the polymer in these regions and to allow pre-polymer to be flushed out immediately after curing. Hydrogels were cured in the devices through the glass substrate by exposure to UV light (360–480 nm) at 7.2 mW cm^{-2} for various durations, depending on the experiment. Immediately after curing, the channel was flushed with 1 mL of supplemented DMEM at a rate of 1 mL min^{-1} to remove uncured pre-polymer solution. Channels were then placed in an incubator (37 °C, 5% CO_2) and perfused with supplemented DMEM at a rate of 1.3 μL min^{-1} using a syringe pump (Cole Palmer, Vernon Hills, IL).

Gel-MA polymerization parameters and cell spreading and viability measurements

Gel-MA macromer concentrations, photoinitiator concentrations, and UV curing times were systematically varied to determine their effects on embedded cell viability. These tests were performed using VICs encapsulated in gel-MA at a final density of 1.5 × 10^6 cells mL^{-1} and cultured in the single layer microchannel devices under constant media perfusion at a rate of 1.3 μL min^{-1} for up to 96 h.

To test the effect of macromer concentration on cell viability, VICs were encapsulated into prepolymer solutions of 5%, 10% and 15% (w/v) gel and 0.5% (w/v) photoinitiator, injected into the microchannels, and cured under UV light (7.2 mW cm^{-2}) for 30 s (5% gel), 25 s (10% gel), and 15 s (15% gel). These were the minimum times required for gel polymerization, as determined by visual inspection. To test the effect of the photoinitiator concentration on cell viability, VICs were mixed in 5% gels with 0.5%, 1% or 2% (w/v) photoinitiator and cured for 30 s. Lower photoinitiator concentrations did not result in complete gel curing in the microchannel, even with up to 10 min of UV exposure. To test the effect of the UV curing time on cell viability, VICs were mixed in 5% gels with 0.5% photoinitiator and UV cured for 30 s, 1 min or 2 min. Lower curing times did not result in complete gel polymerization in the microchannel.

Cell viability was assessed by staining the VICs in the microchannels with a solution of 2 μM calcein AM and 4 μM ethidium homodimer. The solution was injected into the channel and incubated at 37 °C for 30 min. VIC-laden gels were washed by flushing the channels twice with PBS for 15 min. The gels were imaged through their whole thickness by confocal microscopy (Nikon Eclipse Ti) using 5 μm slices that were then combined to reconstruct a 3D z-stack volume. Images were analysed in ImageJ by applying consistent thresholds to the green and red channels to identify live and dead cells, respectively. The number of live and dead cells was determined in three random regions of interest (ROI) per condition. Percent viability was calculated as the number of live cells divided by the total number of cells. Cell spreading was assessed qualitatively based on the calcein AM images.

VEC-VIC co-culture in 3D membrane microfluidic devices under fluid flow-induced shear stress

The upper and lower channels of the membrane microfluidic devices were rinsed sequentially with 100% ethanol, 70% ethanol and sterile PBS. The top channel was then coated with 200 μL of 100 μg mL^{-1} bovine plasma fibronectin and incubated for 1 h at room temperature. VICs were encapsulated in 5% gel-MA with 0.5% photoinitiator at a density of 1.5 × 10^6 cells mL^{-1}, injected into the bottom S-shaped channel, and UV cured for 30 s (Fig. 1C). The top channel was then flushed with 1 mL of M199, supplemented with 10% FBS and

Published on 12 March 2013. Downloaded by University of Toronto on 04/06/2013 21:33:14.

1% P–S, to remove unbound fibronectin. VECs (passage 4; isolated as described previously[16]) were injected into the top channel at a density of 1.5×10^6 cells mL^{-1}, incubated for 4–6 h to allow the VECs to attach to the membrane, and then flushed with 500 μL of supplemented M199 to remove unbound VECs. VECs in the top channel were perfused with 1 mL of supplemented M199 every 12–16 h afterwards. To preserve VIC viability in gel-MA during culture, the bottom channel was perfused constantly with supplemented DMEM at a rate of 1.3 μL min^{-1} *via* a syringe pump (Harvard Apparatus) during which time the inlet and outlet ports of the top channel were connected to one another using polyethylene tubing to prevent non-diffusive flow into the top channel. These culture conditions were maintained for 72 h, after which perfusion of the VICs in the bottom channel was terminated and the VECs in the top channel were exposed to shear stress *via* a recirculatory flow loop inside a 37 °C, 5% CO_2 incubator.[8] Briefly, a peristaltic pump (Cole Palmer, Vernon Hills, IL) was used to drive culture media from a reservoir into a damper. The damper converted the pulsatile flow generated from the pump to a continuous flow entering the top channel. The total volume of culture media used in the recirculatory flow loop was 30 mL. During recirculatory flow, the inlet and outlet ports of the bottom channel were connected to one another using polyethylene tubing (Becton Dickinson) to prevent non-diffusive flow into the bottom VIC channel (*i.e.*, VIC-laden gels in the bottom channel were maintained under no flow conditions). Top channel VECs were subjected to steady flow-induced shear stress of 20 dyn cm^{-2} or 0 dyn cm^{-2} (static) for 24 h. For the static condition, VEC culture media was replaced in the top channel every 12 h.

Cell staining and imaging

In some experiments, VICs and VECs were fluorescently labelled prior to seeding with CellTracker™ Red CMTPX or Green CMFDA (Life Technologies, Burlington, ON, Canada) vital cell dyes, respectively, according to the manufacturer's instructions.

To stain VICs for α-smooth muscle actin (α-SMA), the PDMS slabs were gently removed and the gel on the glass slides was transferred into multiwell plates. VICs were fixed with 10% neutral buffered formalin for 24 h at 4 °C and then permeabilized with 0.1% Triton X100 for 15 min. They were then washed with PBS for 10 min and blocked with 3% bovine serum albumin (BSA) for 25 min at 37 °C. Subsequently, samples were stained for 90 min at 37 °C with Cy3-conjugated monoclonal mouse anti-human α-SMA antibody diluted in 3% BSA in a 1 : 100 ratio. Samples were then washed with PBS and stained for nuclei with 1 μg mL^{-1} Hoechst dye in PBS for 8 min, and washed with PBS for 10 min.

To visualize f-actin in VECs, samples were stained with 1 μg mL^{-1} phalloidin-fluorescein isothiocyanate in 3% BSA for 60 min at room temperature, washed with PBS for 10 min and then imaged within the device.

Samples were imaged using a confocal microscope, with image slices taken every 5 μm and then combined to form a 3D z-stack volume. Myofibroblasts were identified as spread (non-circular) cells that had α-SMA fluorescent intensity above a minimum threshold, which was set to the same value for all images. The total number of cells was obtained by using the corresponding nuclear stained images. Cells were counted in three ROI per condition.

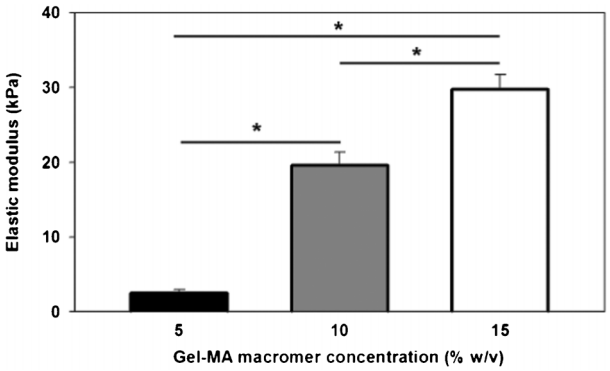

Fig. 2 Compressive elastic moduli of gel-MA hydrogels as a function of macromer concentration (*$p < 0.001$).

Statistical analyses

Data are presented as mean ± standard deviation ($n = 3$ samples per condition in all cases). Comparisons were made by one-way ANOVA with pairwise comparisons by the Tukey test. All statistical analyses were performed using SigmaStat 3.5 (Systat Software Inc., San Jose, CA).

Results

Gel-MA mechanical characterization

The elastic modulus and porosity of the gel-MA hydrogels varied as a function of the macromer concentration, as expected. The elastic moduli ranged from 2.5 kPa (5% w/v gel) to ~30 kPa (15% w/v gel) ($p < 0.001$ between each macromer concentration; Fig. 2), with no sample failing before the maximum load of 30 g was reached. Average pore sizes decreased significantly with increasing macromer concentration from 20 μm (5% w/v gel) to 7 μm (15% w/v) ($p < 0.05$ between each macromer concentration; Fig. 3). The morphology of the pores also differed with macromer concentration: pores in the 5% gels were more heterogeneous in size and distribution throughout the gel, but were interconnected (Fig. 3A,B), whereas the 15% gels had uniformly sized and distributed closed pores separated by thin walls (Fig. 3D).

Effect of gel polymerization conditions on cell viability and spreading

Gel polymerization conditions were systematically investigated to identify conditions that best supported cell viability. Macromer concentration had no significant influence on cell viability, with over 84% viability after four days of culture for all gels ($p > 0.17$; Fig. 4A,B).

Qualitatively, VICs were more spread in the 5% gels than in the 10% and 15% gels, and became more spread with time in culture (Fig. 4A). Cell viability decreased in a dose-dependent manner with increasing photoinitiator concentration ($p < 0.05$

 This journal is © The Royal Society of Chemistry 2013

Published on 12 March 2013. Downloaded by University of Toronto on 04/06/2013 21:33:14.

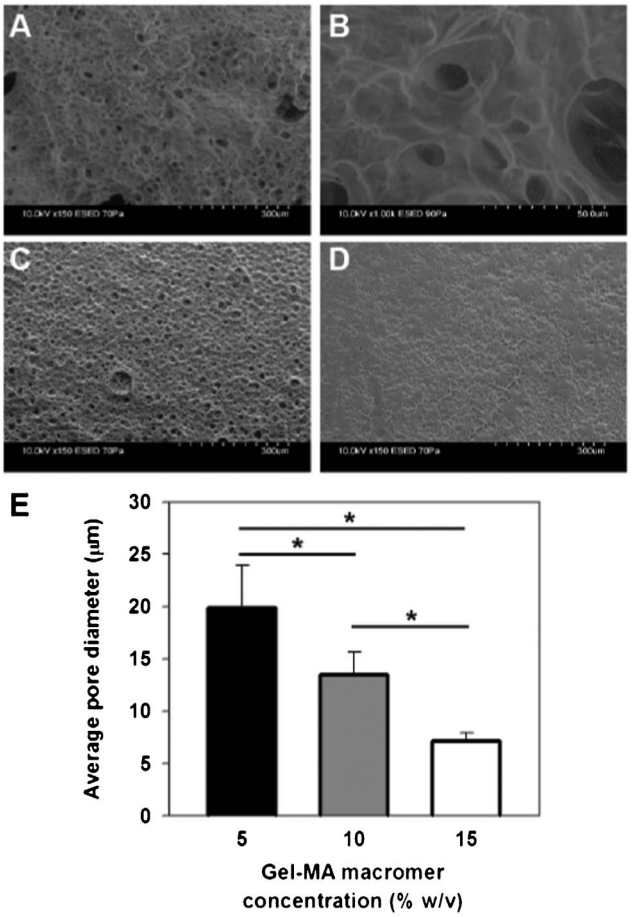

Fig. 3 Environmental scanning electron micrographs showing the porosity of (A) 5% gel-MA (150X); (B) 5% gel-MA (1000X); (C) 10% gel-MA (150X); and (D) 15% gel-MA (150X) hydrogels. (E) Average pore diameters for different gel-MA macromer concentrations (*$p < 0.05$).

between each photoinitiator concentration; Fig. 4C,D), from 94% viability with 0.5% photoinitiator to complete cell death with 2% photoinitiator. Cell spreading also decreased with increasing photoinitiator concentration (Fig. 4C). Cell viability and spreading were similar with UV exposure times of 30 s, 1 min, and 2 min after 24 h of culture ($p = 0.52$; Fig. 4E,F). However, after 48 h of culture, viability decreased with increasing UV exposure time ($p < 0.05$ between each exposure time; Fig. 4E,F) and cells were less spread in the 15% gels than in the other two (Fig. 4E).

Effect of VEC co-culture and shear stress on VIC myofibroblast differentiation

To demonstrate the utility of the membrane microfluidic platform to study cell-cell interactions under physiologically relevant conditions, we co-cultured a monolayer of VECs on the porous membrane of the upper channel and VICs embedded in a gel-MA hydrogel in the lower channel. After three days of co-culture in the membrane device, VECs in the top channel formed a confluent monolayer with a characteristic cobblestone appearance and VICs were well spread in the gel-MA in the lower channel, with minimal α-SMA expression. Pre-labelling of the VICs and VECs with fluorescent vital dyes confirmed that no cross-contamination occurred between the upper and lower channels (Fig. 5). VECs were then subjected to 0 or 20 dyn cm^{-2} flow-induced shear stress for 24 h. After application of flow, VECs remained viable, demonstrated some elongation but without obvious preferential orientation, and remained in the upper channel (Fig. 6A,B). We assessed paracrine interaction between the VECs and VICs under static and flow conditions by counting the proportion of α-SMA-positive VICs as a measure of myofibroblast differentiation (Fig. 6C–F). The proportion of α-SMA-positive myofibroblasts was highest at 78% when VICs were cultured alone, without VECs in the upper channel. The proportion of myofibroblasts decreased significantly to 29% when VECs were present and cultured under static conditions ($p < 0.001$ *vs.* no VEC condition), but was the lowest at 17% when the VECs were subjected to shear stress ($p < 0.001$ *vs.* no VEC condition; $p = 0.066$ *vs.* static VEC condition).

Discussion

While microfluidics has been applied successfully to model and study microcirculatory phenomena, microfluidic platforms that model larger blood vessels and heart valves are lacking. This is despite the clear benefits that microfluidics offer for cell culture technologies, including the potentials for improved physiological relevance and enhanced throughput. To address this need, we developed a bilayer membrane microfluidic device that mimics critical features of vascular and valvular 3D microenvironments. Key features of the platform include: (1) a porous membrane that permits cell-cell interactions and transendothelial extravasation[8] while compartmentalizing heterotypic cell types to maintain a physiological EC monolayer and facilitate cell type-specific isolation and analyses; (2) the application of flow-induced shear stress in a physiologically relevant configuration; (3) direct incorporation of a mechanically stable and tunable hydrogel to mimic the mural space; (4) a high degree of encapsulated cell viability over several days of culture; and (5) being amenable to parallelization to increase throughput. Here we demonstrated the utility of the platform to model endothelial paracrine regulation of VIC phenotype, but it should have broad utility to model EC-mural cell interactions in other cardiovascular tissues.

An important component of the platform presented here was the use of gel-MA to recapitulate the 3D subendothelial ECM. Gel-MA provides the cell-interactive and -responsive aspects of native collagen, but as shown here, remained intact for a period of several days despite being populated with a high density of contractile and synthetic cells. Further, the gel-MA stiffness is tunable within the physiological range of most soft tissues;[17] for example, the elastic moduli of the aortic valve range from 1 to 21 kPa.[18,19] ECM stiffness is an important regulator of vascular smooth muscle and VIC responses, including migration,[20] responsiveness to growth factors,[19] and cell fate,[15,21] and thus it is important to able to

Published on 12 March 2013. Downloaded by University of Toronto on 04/06/2013 21:33:14.

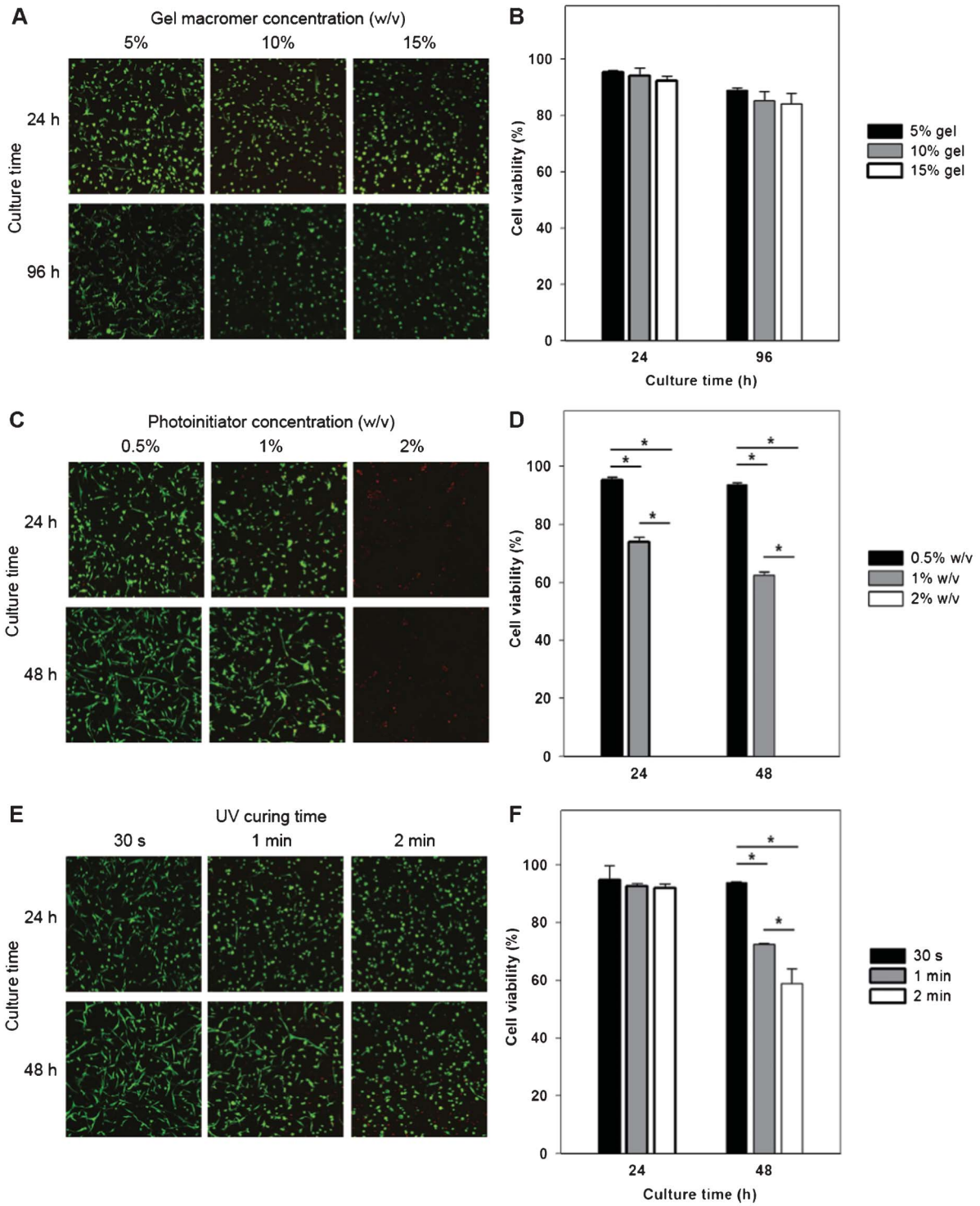

Fig. 4 Cell viability in gel-MA hydrogels as functions of (A, B) macromer concentration, (C, D) photoinitiator concentration, and (E, F) UV curing time (*$p < 0.05$). See text for details of polymerization parameters.

tune the ECM mechanical properties to closely mimic the *in vivo* environment. While we demonstrated control of gel stiffness through the macromer concentration, additional control can be achieved by modifying the extent of methacrylation.[10]

The microfluidic device design and processing parameters we identified enabled photopolymerization of the gel-MA directly in the microchannels with higher viability of primary cells than is typically achieved in other microphotopatterned gels, even with robust cell lines.[22,23] Further improvements in

 This journal is © The Royal Society of Chemistry 2013

Published on 12 March 2013. Downloaded by University of Toronto on 04/06/2013 21:33:14.

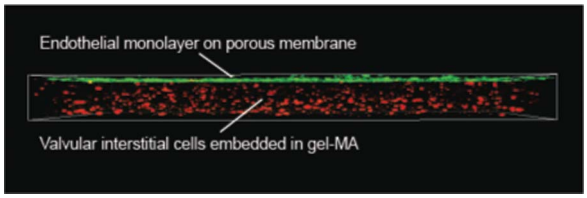

Fig. 5 Perspective view of a 3D confocal reconstruction demonstrating the compartmentalization and spatial arrangement of fluorescently-labelled cells in the bilayer membrane microfluidic platform after three days of co-culture. VECs (green) form a monolayer on the porous membrane in the upper channel and VICs (red) are distributed throughout a 5% (w/v) gel-MA 3D hydrogel in the lower channel.

cell viability may be achieved by using more hydrophilic photoinitiators that are less likely to intercalate in the hydrophobic cell membrane[24] or antioxidants or surfactants that protect against UV damage.[25] These strategies may be particularly important if higher photoinitiator concentrations are used for additional control of gel-MA porosity, as has been shown previously.[10] It is notable that VIC viability was not affected by the macromer concentration, despite significant differences in porosity and microarchitecture (Fig. 4A,B). Although the 15% gel pores appeared closed, all gels were perfusable, suggesting that there was interconnectivity between pores in the cell-laden gels. The high viability of the VICs in all of the gels was likely due to their perfusability and because the cells were able to partially degrade the gel-MA over time to enable spreading.

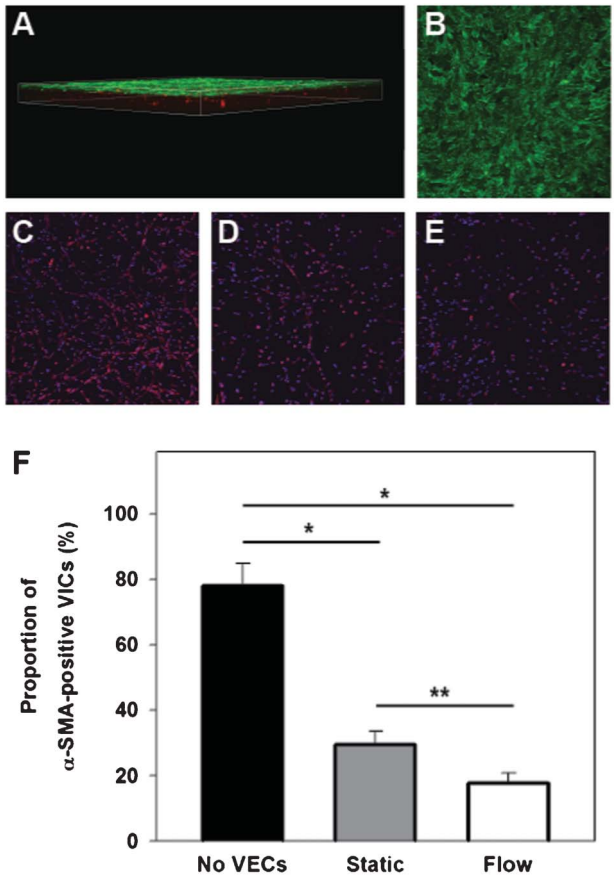

Fig. 6 (A) Perspective view of a 3D confocal reconstruction of the membrane microfluidic device after 24 h of shear stress application. The endothelial monolayer (stained green for f-actin) remained intact and separate from α-SMA-positive VICs (red) in the 5% (w/v) gel-MA hydrogel in the lower channel. (B) En face view of VECs (stained for f-actin) after shear stress application (bottom-to-top in this image). (C–E) VICs stained for α-SMA (red) and nuclei (blue) after: (C) culture without VECs or fluid flow; (D) co-culture with VECs grown statically; and (E) co-culture with VECs subjected to 20 dyn cm^{-2} shear stress for 24 h. (F) Quantification of the proportion of α-SMA-positive VICs (myofibroblasts) in the hydrogels under various co-culture and shear stress conditions (*$p < 0.001$; **$p = 0.066$).

As proof-of-principle, we applied the microfluidic platform to model the heart valve microenvironment. *In vivo*[12] and *in vitro*[6] studies suggest that hemodynamically-regulated paracrine communication between VECs and VICs may contribute to homeostasis and focal lesion development in the aortic valve. Our platform enabled VECs to be subjected to shear stress while maintaining underlying VICs in a non-sheared 3D environment with physiological mechanical properties. We found that VECs suppress VIC myofibroblast differentiation, and that shear stress enhances this effect. Importantly, these results are consistent with those observed by Butcher *et al.* using a macroscale tissue-engineered model,[13] thus confirming the *in vitro* fidelity of the microfluidic culture system. The shear dependency of VIC myofibroblast differentiation is also consistent with *in vivo* observations of diseased valves, which demonstrate fibrosis and calcification preferentially on the aortic side of the leaflet in regions with low shear stresses,[12] supporting the physiological fidelity of the microfluidic platform. The paracrine factor(s) produced by VECs to regulate VICs have not been identified, but nitric oxide (NO) may be involved, as it is upregulated in ECs by shear stress[26] and inhibits VIC myofibroblast activation under static conditions *in vitro*.[27] Another candidate is C-type natriuretic peptide (CNP), which we discovered is expressed by VECs only in high shear stress regions of the aortic valve[12] and showed inhibits VIC pathological differentiation *in vitro*.[28] Because the microenvironment and cellular constituents can be precisely controlled and probed in the microfluidic platform, it is well-suited to investigate the signalling mechanisms involved in bidirectional VEC-VIC communication. With parallelization, the platform should also be useful for drug screening and toxicity studies.[29] While the current configuration mimics the valvular microenvironment much better than standard tissue culture technologies, physiological fidelity could be improved in the future by applying complex shear stress waveforms[30–32] and by incorporating deformable substrates that mimic valve tissue deformation.[33,34]

Conclusions

A membrane microfluidic platform was developed to mimic the vascular/valvular 3D microenvironment, including fluid flow over an endothelial monolayer, a porous membrane that

Published on 12 March 2013. Downloaded by University of Toronto on 04/06/2013 21:33:14.

permits heterotypic cell interactions while maintaining cell compartmentalization, and a mechanically tunable gel-MA hydrogel as a physiologically-relevant subendothelial 3D matrix that support long-term cell viability. In proof-of-principle experiments, the presence of VECs suppressed VIC pathological differentiation to α-SMA-expressing myofibroblasts, an effect that was enhanced when the endothelium was exposed to flow-induced shear stress. These responses in the microfluidic platform are similar to those of conventional macroscale systems, while offering the advantages of greater control of the cellular microenvironment and the potential for higher throughput experimentation. We expect this versatile organ-on-a-chip platform to have broad utility for mechanistic vascular and valvular biology studies and with parallelization, to be useful for drug screening in physiologically-relevant 3D microenvironments.

Acknowledgements

We thank Zahra Mirzaei, Laura-lee Caruso, Bogdan Beca, and Jenna Usprech for expert technical assistance, and Dr. Jason Nichol, Shahed Al-Haque, and Dr. Ali Khademhosseini (Massachusetts Institute of Technology) for assistance with gel-MA synthesis. This study was supported by a Collaborative Health Research Project grant from the Natural Science and Engineering Research Council (NSERC) of Canada and the Canadian Institutes of Health Research (Grant No. CHRP 385956-2010); an NSERC Undergraduate Student Research Award (to M.B.C.); an NSERC Canada Graduate Scholarship (to S.S.); and the Canada Research Chairs in Bioanalytical Chemistry (to A.R.W.) and Mechanobiology (to C.A.S.).

Notes and references

1 D. Huh, Y. S. Torisawa, G. A. Hamilton, H. J. Kim and D. E. Ingber, *Lab Chip*, 2012, **12**, 2156–2164.
2 E. W. Young and C. A. Simmons, *Lab Chip*, 2010, **10**, 143–160.
3 K. H. Wong, J. M. Chan, R. D. Kamm and J. Tien, *Annu. Rev. Biomed. Eng.*, 2012, **14**, 205–230.
4 P. F. Davies, *Physiol. Rev.*, 1995, **75**, 519–560.
5 P. Sucosky, K. Balachandran, A. Elhammali, H. Jo and A. P. Yoganathan, *Arterioscler., Thromb., Vasc. Biol.*, 2009, **29**, 254–260.
6 J. T. Butcher, S. Tressel, T. Johnson, D. Turner, G. Sorescu, H. Jo and R. M. Nerem, *Arterioscler., Thromb., Vasc. Biol.*, 2006, **26**, 69–77.
7 E. W. Young, M. W. Watson, S. Srigunapalan, A. R. Wheeler and C. A. Simmons, *Anal. Chem.*, 2010, **82**, 808–816.
8 S. Srigunapalan, C. Lam, A. R. Wheeler and C. A. Simmons, *Biomicrofluidics*, 2011, **5**, 13409.
9 J. W. Nichol, S. T. Koshy, H. Bae, C. M. Hwang, S. Yamanlar and A. Khademhosseini, *Biomaterials*, 2010, **31**, 5536–5544.
10 J. A. Benton, C. A. DeForest, V. Vivekanandan and K. S. Anseth, *Tissue Eng. A*, 2009, **15**, 3221–3230.
11 N. M. Rajamannan, F. J. Evans, E. Aikawa, K. J. Grande-Allen, L. L. Demer, D. D. Heistad, C. A. Simmons, K. S. Masters, P. Mathieu, K. D. O'Brien, F. J. Schoen, D. A. Towler, A. P. Yoganathan and C. M. Otto, *Circulation*, 2011, **124**, 1783–1791.
12 C. A. Simmons, G. R. Grant, E. Manduchi and P. F. Davies, *Circ. Res.*, 2005, **96**, 792–799.
13 J. T. Butcher and R. M. Nerem, *Tissue Eng.*, 2006, **12**, 905–915.
14 C. Moraes, Y. Sun and C. A. Simmons, *J. Micromech. Microeng.*, 2009, **19**, 065015.
15 C. Y. Yip, J. H. Chen, R. Zhao and C. A. Simmons, *Arterioscler., Thromb., Vasc. Biol.*, 2009, **29**, 936–942.
16 W.-Y. Cheung, E. W. Young and C. A. Simmons, *Journal of Heart Valve Disease*, 2008, **17**, 674–681.
17 A. Buxboim, I. L. Ivanovska and D. E. Discher, *J. Cell Sci.*, 2010, **123**, 297–308.
18 R. Zhao, K. L. Sider and C. A. Simmons, *Acta Biomater.*, 2011, **7**, 1220–1227.
19 J. H. Chen, W. L. Chen, K. L. Sider, C. Y. Yip and C. A. Simmons, *Arterioscler., Thromb., Vasc. Biol.*, 2011, **31**, 590–597.
20 S. R. Peyton and A. J. Putnam, *J. Cell. Physiol.*, 2005, **204**, 198–209.
21 S. R. Peyton, P. D. Kim, C. M. Ghajar, D. Seliktar and A. J. Putnam, *Biomaterials*, 2008, **29**, 2597–2607.
22 C. Moraes, G. Wang, Y. Sun and C. A. Simmons, *Biomaterials*, 2010, **31**, 577–584.
23 P. Panda, S. Ali, E. Lo, B. G. Chung, T. A. Hatton, A. Khademhosseini and P. S. Doyle, *Lab Chip*, 2008, **8**, 1056–1061.
24 S. J. Bryant, J. L. Cuy, K. D. Hauch and B. D. Ratner, *Biomaterials*, 2007, **28**, 2978–2986.
25 V. A. Liu and S. N. Bhatia, *Biomed. Microdevices*, 2002, **4**, 257–266.
26 J. P. Cooke, *Proc. Natl. Acad. Sci. U. S. A.*, 2003, **100**, 768–770.
27 J. A. Kennedy, X. Hua, K. Mishra, G. A. Murphy, A. C. Rosenkranz and J. D. Horowitz, *Eur. J. Pharmacol.*, 2009, **602**, 28–35.
28 C. Y. Yip, M. C. Blaser, Z. Mirzaei, X. Zhong and C. A. Simmons, *Arterioscler., Thromb., Vasc. Biol.*, 2011, **31**, 1881–1889.
29 P. Neuzi, S. Giselbrecht, K. Lange, T. J. Huang and A. Manz, *Nat. Rev. Drug Discovery*, 2012, **11**, 620–632.
30 S. Chandra, N. M. Rajamannan and P. Sucosky, *Biomech. Model. Mechanobiol.*, 2012, **11**, 1085–1096.
31 C. H. Yap, N. Saikrishnan, G. Tamilselvan and A. P. Yoganathan, *Biomech. Model. Mechanobiol.*, 2012, **11**, 171–182.
32 C. H. Yap, N. Saikrishnan and A. P. Yoganathan, *Biomech. Model. Mechanobiol.*, 2012, **11**, 231–244.
33 C. Moraes, J. H. Chen, Y. Sun and C. A. Simmons, *Lab Chip*, 2010, **10**, 227–234.
34 J. Zhou and L. E. Niklason, *Integr. Biol.*, 2012, **4**, 1487–1497.

 This journal is © The Royal Society of Chemistry 2013